coatings

MDPI

Article

Investigation of Polystyrene-Based Microspheres from Different Copolymers and Their Structural Color Coatings on Wood Surface

Yi Liu [1,2,*] and Jing Hu [1,2]

[1] College of Furnishings and Industrial Design, Nanjing Forestry University, Nanjing 210037, China; hj_nanlin2019@126.com
[2] Jiangsu Co-Innovation Center of Efficient Processing and Utilization of Forest Resources, Nanjing Forestry University, Nanjing 210037, China
* Correspondence: liuyi@njfu.edu.cn; Tel.: +86-25-8542-7528

Abstract: Six kinds of polystyrene (PSt)-based colloidal microspheres were synthesized by adding acrylic acid (AA), methyl methacrylate (MMA), and butyl acrylate (BA) as comonomers in styrene emulsion polymerization. The structurally colored coatings on a wood surface were self-assembled by thermally assisted gravity deposition of these microspheres. Chemical compositions and structures of microspheres and morphological characteristics of microspheres and structural color coatings, as well as optical properties of coatings and their generated structural colors, were studied. Pure PSt microspheres had a smooth surface and uniform structure, while microspheres of copolymers had core–shell morphologies and a rough surface. Only poly(styrene-acrylic acid) (P(St-AA)) microspheres had good monodispersity and the resulting coating had a well-ordered photonic crystal structure. However, other kinds of microspheres could form short ranges of ordered amorphous photonic crystal structures and they displayed structural colors. Both the reflectivity of coatings to visible light and structural colors varied with microsphere size and self-assembly temperature.

Keywords: polystyrene; microsphere; copolymer; wood; structural color

check for updates

Citation: Liu, Y.; Hu, J. Investigation of Polystyrene-Based Microspheres from Different Copolymers and Their Structural Color Coatings on Wood Surface. *Coatings* **2021**, *11*, 14. https://dx.doi.org/10.3390/coatings11010014

Received: 2 December 2020
Accepted: 21 December 2020
Published: 25 December 2020

Publisher's Note: MDPI stays neutral with regard to jurisdictional claims in published maps and institutional affiliations.

Copyright: © 2020 by the authors. Licensee MDPI, Basel, Switzerland. This article is an open access article distributed under the terms and conditions of the Creative Commons Attribution (CC BY) license (https://creativecommons.org/licenses/by/4.0/).

1. Introduction

Wood is a natural organic composite material, which is rich in resources, renewable, and clean, and is widely used in architecture, decoration, and furniture [1,2]. When used as a decorative material, the natural color and texture of wood impart a psychologically good feeling. Wood is a product of tree growth, and it has various types of natural defects. Taking into account these defects, researchers have adopted various methods to improve the functionality of wood. In the processing and utilization of wood, surface decoration can help in adjusting the wood color, changing its surface physical and chemical properties, and making up for its natural defects, thus expanding the scope of applications of wood [3,4]. Artificial coloration of wood surfaces is an extremely important step in wood decoration technology. Presently, the main methods to improve wood color are dyeing and induced discoloration [5,6]. However, the shortcomings of the wood dyeing process are wastage of dyes and environmental pollution. Sometimes, discoloration cannot be controlled and the color of treated wood may become uneven or fade away [7–10]. Therefore, fundamentally new methods to solve environmental factors and fading problems of wood color improvement are required.

Instead of changing the color of wood using dyes, structural coloration is another feasible method, which is inspired by biological colors in nature [11,12]. Structural coloration is a physical phenomenon of color generation with photonic structures. The color produced by interactions between light and physical structures has the same magnitude as wavelengths of light [13]. Different from pigments, structural coloration is a phenomenon involving refraction, diffuse reflectance, diffraction, or interference of light waves, caused

by microscopic structures of objects, resulting in optical effects with specific colors [14]. If the microstructure does not undergo changes, the optical effects do not disappear. Therefore, compared with coloration by pigmentation, structural coloration has the advantage of resistance to fading. The structural color of living or inanimate objects can be mainly attributed to their photonic crystal structure [15–17]. Photonic crystal is a material with periodic variations of dielectric constant, and there are many varieties. The three-dimensional structure of photonic crystal is most complex [18]. The most typical representative of a three-dimensional photonic crystal in nature is opal. Studies on the structures of photonic crystals found in nature have inspired the syntheses of various artificial bionic structural colored materials [12,19].

The photonic crystal structures are usually prepared by "top-down" and "bottom-up" methods. Photonic crystal is formed by the self-assembly of monodisperse colloidal particles in the "bottom-up" method [20]. In the self-assembly process, colloidal particles in the dispersant form well-ordered photonic crystals due to van der Waals forces, electrostatic repulsion, gravity, capillary force, etc. [21]. Monodisperse particles, the building blocks of colloidal photonic crystals, can be categorized as inorganic or organic. The most commonly used inorganic particles are SiO_2 microspheres [22,23], whereas polystyrene is the most commonly used organic raw material [24,25]. At present, emulsion polymerization, soap-free emulsion polymerization, seed emulsion polymerization, suspension polymerization, dispersion polymerization, etc., are commonly used methods for the preparation of polystyrene (PSt) microspheres. PSt microspheres obtained by these polymerization methods differ in particle size and uniformity. The PSt microspheres obtained by emulsion polymerization display good monodispersity, wherein their diameters range from tens to hundreds of nanometers [16,24]. For a photonic crystal composed of microspheres, particle sizes of microsphere units should conform to Bragg's diffraction, which is about 170–370 nm. Submicron-sized PSt microspheres synthesized by emulsion polymerization are suitable structural units for self-assembly in the formation of photonic crystals.

PSt microspheres are typically hard, due to which photonic crystal structures formed from PSt microspheres are bonded only by molecular forces, and their performance is poor. With the addition of comonomers in the polymerization process, flexible materials can be uniformly coated on the surface of PSt to form colloidal microspheres with a core–shell morphology [26]. Acrylate and acrylic acid are typically used in the copolymerization of PSt [27]. If the structure, size, and composition of the shell portions of microspheres are controlled, interactions between microspheres can be adjusted. The flexibility of microspheres increases, due to which the dispersion stability of microspheres in the medium improves. By changing the parameters of the well-ordered structure of photonic crystals, the saturation of structural color can be improved [28–34]. In this study, acrylic acid (AA), methyl methacrylate (MMA), and butyl acrylate (BA) were used as copolymers in the polymerization reactions with styrene (St). Properties of the synthesized microspheres and photonic crystals constructed by the self-assembly of microspheres were studied to determine the influence of copolymers on PSt microspheres and structural color coatings on a wood surface.

2. Materials and Methods

2.1. Materials and Substrates

St, AA, MMA, BA, and the emulsifier (sodium dodecyl benzene sulfonate (SDBS)) were purchased from Shanghai Lingfeng Chemical Reagent Co. Ltd. (Shanghai, China). Ammonium persulfate (APS) (initiator) and absolute ethyl alcohol (dispersion medium) were purchased from Nanjing Chemical Reagent Co. Ltd. (Nanjing, China). These reagents were chemically pure and were used without further purification. Deionized water was used in the polymerization reactions. The wood species aspen (*Populus tremuloides*), used to construct surface photonic crystals, was purchased from the local market. Wood was cut into small pieces of dimensions of 50 mm (radial) × 40 mm (longitudinal) × 10 mm (tangential), and the surface was sanded using 320-mesh sandpaper, and the dust produced

by sanding was cleaned with a brush and compressed air. The surface of the wood used to construct the photonic crystal was a radial section which had several parallel linear textures and a fine xylem ray.

2.2. Synthesis of Polystyrene Microspheres

Six sets of PSt-based colloidal microspheres were synthesized using different combinations of monomers by emulsion polymerization, the details of which are shown in Table 1. For example, the polymerization of P(St-MMA-AA) microspheres was carried out in a three-necked round-bottomed flask, equipped with a mercury thermometer, mechanical stirrer, and condenser tube. Deionized water (100 mL), absolute ethanol (40 mL), SDBS (0.2 g), and APS (0.15 g) were successively added into the flask. The reaction was stirred at 400 rpm. The reagent mixture was heated to 70 °C in a water bath. Then St (19 g), MMA (1 g), and AA (1 g) were added to the reaction vessel. The emulsion polymerization was continued for 6 h.

Table 1. Experimental details of different polystyrene (PSt)-based colloidal microspheres synthesized by emulsion polymerization.

Target Colloidal Microspheres	St (g)	AA (g)	MMA (g)	BA (g)	Deionized Water (mL)	Ethanol (mL)	SDBS (g)	APS (g)
PSt	19	–	–	–	100	40	0.2	0.15
P(St-AA)		1	–	–				
P(St-MMA-AA)		1	1	–				
P(St-MMA)			1	–				
P(St-BA-AA)		1	–	1				
P(St-BA)		–	–	1				

2.3. Preparation of Structural Color Coatings on a Wood Surface Using PSt-Based Microspheres

PSt-based microspheres were self-assembled on the wood surface by the thermally assisted gravity deposition method that formed photonic crystals with structural color. Before self-assembly, a wire frame with an area of 35 mm × 35 mm was drawn with a pencil on the wood radial section after sanding. Then, 10 wt.% emulsion containing different PSt-based colloidal microspheres was dropped into the wire frame, 0.6 mL each time. Thereafter, the wood covered with emulsion was placed in a drying oven, and different samples were set at different temperatures of 40, 50, 60, and 70 °C. The samples were dried for 2 h, to ensure complete drying of final photonic crystals.

2.4. Characterization

Morphologies of six kinds of PSt-based colloidal microspheres were studied by transmission electron microscopy (TEM, JEM2100F, JEOL, Akishima-shi, Japan). X-ray photoelectron spectroscopy (XPS, AXIS Ultra DLD, Kratos, Manchester, UK) was used to determine the chemical compositions of various microspheres. High-resolution spectra (C1s and O1s) at binding energies from 279 to 299 eV and 525 to 546 eV for C and O, respectively, were obtained. Functional groups of microspheres were determined by attenuated total reflectance Fourier transform infrared spectroscopy (ATR-FTIR, Alpha II, Bruker, Berman, Germany). Photonic crystals formed by self-assembly of microspheres on the wood surface were characterized by field emission scanning electron microscopy (FESEM, Quanta 400 FEG, FEI, Hillsboro, OR, USA). Reflectance spectra of photonic crystal coatings on the wood surface were acquired using a UV–Vis spectrometer (Lambda 950, Perkin-Elmer, Waltham, MA, USA) in a visible light region. A digital camera (d7000, Nikon, Tokyo, Japan) was used to photograph the structural colors of photonic crystals on the wood surface under white light illumination.

3. Results and Discussion

3.1. Effect of Copolymers on Properties of PSt-Based Microspheres

3.1.1. XPS Spectroscopic Analysis of Microspheres of PSt with Different Copolymers

The elemental composition of six types of PSt-based colloidal microspheres formed by emulsion polymerization was analyzed by XPS, as shown in Figure 1. The wide-scan spectra (Figure 1a) of different PSt-based microspheres showed similar peaks. Peaks at 284 and 533 eV could be assigned to C and O, respectively. Peaks at 1228 and 978 eV were Auger peaks of the two elements. These were seen as the most obvious peaks in the spectra. The result of XPS wide-scan spectra was in accordance with some previous studies [35,36]. For the five kinds of microspheres obtained by copolymerization of AA, MMA, and BA with St, the presence of peaks for oxygen was not surprising, since these substances contained carboxyl (–COOH) or ester (–COOR) groups. Pure PSt ($(C_8H_8)_n$) has no oxygen in it. Hence, it was speculated that the peak of oxygen in PSt microspheres was due to SO_4 in the initiator APS, sulfonyl ($–S(=O)_2–$) in the emulsifier SDBS, and other oxygen impurities. Therefore, compared with the other five kinds of microspheres, the intensities of 533 and 978 eV peaks of PSt microspheres were the lowest. In wide-scan spectra, two peaks at 169 and 1072 eV could be ascribed to sulfur and sodium present in APS and SDBS, indicating that microspheres in the emulsion were composed of polymer, initiator, and emulsifier after polymerization. They may also contain unreacted monomers. The initiator APS produced initial sulfate free radicals under thermal action. The initial radical reacted with the monomer to form a monomer radical, then the molecular chain grew to form macromolecules. The sulfate radical bound to the end of the macromolecular chain. The emulsifier SDBS contained both hydrophilic and oleophilic groups that do not participate in polymerization. During the reaction, the oleophilic group went inside the monomer droplet while the hydrophilic group remained in the aqueous phase. SDBS is a typical anionic emulsifier, and would distribute around surface of microspheres to make it negative and ensure the formation of a stable emulsion system. Both APS and SDBS played a significant role in the resulting coating properties, such as adhesion and wettability [35].

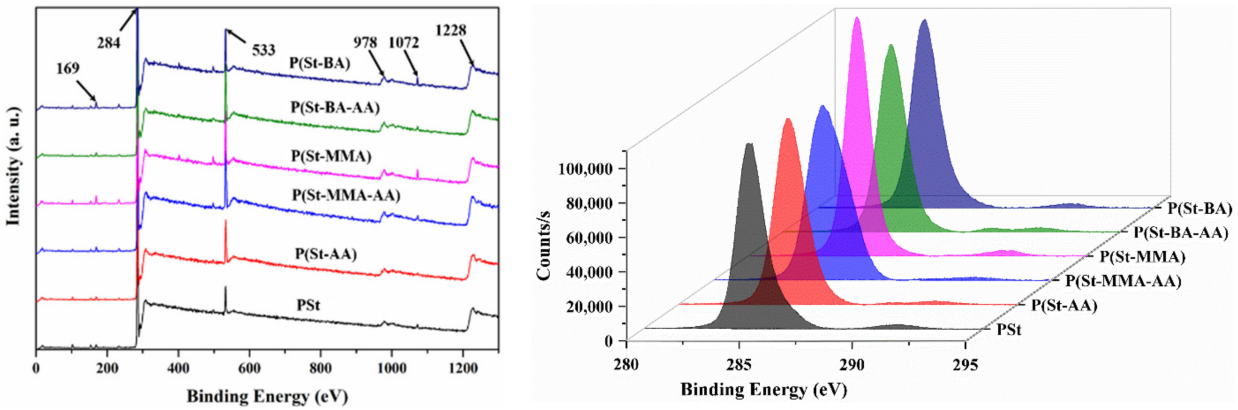
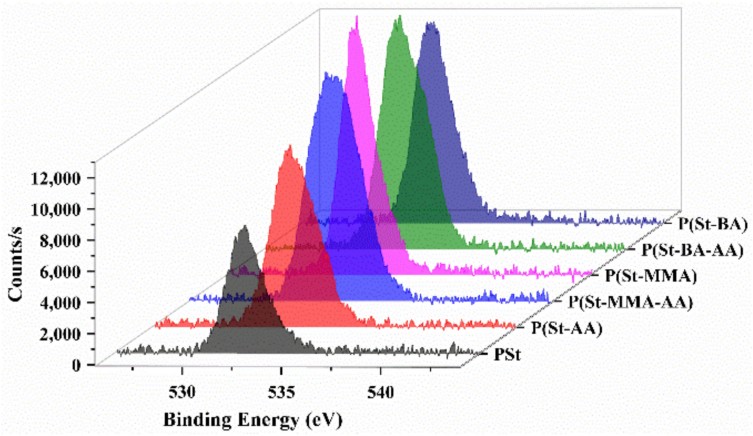


Figure 1. *Cont.*



(**c**)

Figure 1. XPS spectra of six types of PSt-based microspheres; (**a**) wide-scan spectra, (**b**) C1s spectra, and (**c**) O1s spectra.

High-resolution C1s and O1s spectra of different PSt-based microspheres were analyzed. In the C1s spectra (Figure 1b), microspheres showed a strong peak and a weak peak at 284.8 and 291.2 eV, respectively. Peaks at 284.8 eV corresponded to the C–C and C–H functional groups in microspheres, while the other peaks at 291.2 eV were satellite peaks, due to π–π shake-up of benzene rings. In addition to these two peaks, the spectra of P(St-AA), P(St-MMA-AA), and P(St-BA-AA) microspheres also showed a weak peak near 289 eV. This implied that the surfaces of these three microspheres had –COOH groups, contributed by AA. Relative strengths of the peaks near 284.8 eV in C1s spectra of P(St-MMA) and P(St-BA) microspheres were significantly higher than those of the others. This suggested that the addition of MMA and BA as copolymers increased the numbers of methyl and methylene groups on branched chains in the microspheres. The C1s spectra results were identical with those of a previous study [37]. In the O1s spectra (Figure 1c), peaks appeared at 533 eV for all kinds of microspheres. Peaks were attributed to C=O, C–O, and C–O–C bonds in carboxyl and ester groups. These two peaks from different microspheres could be obtained by the deconvolution of O1s spectra. The O1s spectra in Figure 2 clearly shows the presence of two types of oxygens at binding energies of 532.2 and 533.6 eV, which could be attributed to oxygen in C=O linkages or C–O or C–O–C linkages, respectively. These peaks were identical to those shown in a previous study [37]. For pure PSt microspheres, peak height and area at 533.6 eV were very small. The peak of oxygen at 532.2 eV corresponded to S–O bonding in SO_4 functional groups.

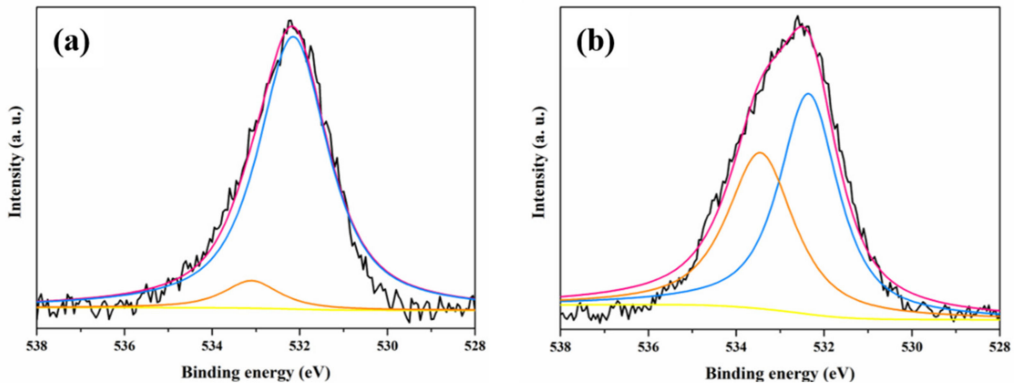


Figure 2. *Cont.*

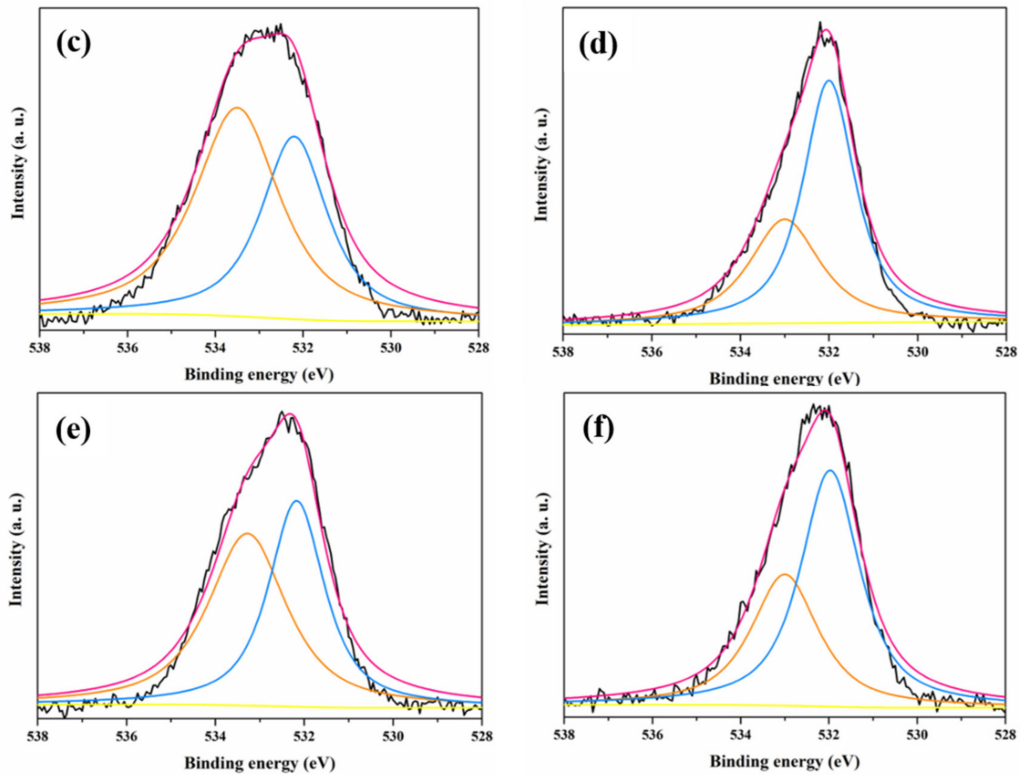


Figure 2. Deconvoluted O1s spectra of six PSt-based microspheres; (**a**) PSt, (**b**) P(St-AA), (**c**) P(St-MMA-AA), (**d**) P(St-MMA), (**e**) P(St-BA-AA), and (**f**) P(St-BA).

3.1.2. FTIR Spectroscopic Analysis of Microspheres of Different PSt Copolymers

The functional groups in colloidal microspheres formed by adding different comonomers were analyzed by FTIR (Figure 3). Peaks at 3025, 3060, and 3081 cm^{-1} were characteristic of C–H bonds in benzene rings. Peaks at 2923 and 2849 cm^{-1} corresponded to the asymmetric and symmetric stretching vibrations of C–H bond in $–CH_2–$, respectively. Peaks at 1601, 1492, and 1451 cm^{-1} were typical skeletal vibrations of benzene rings. Due to the conjugation effects, a peak at 1582 cm^{-1} appeared. A peak at 1372 cm^{-1} could be ascribed to the bending vibrations of the C–H bond in $–CH_3$. Peaks at 1028 and 1067 cm^{-1} reflected the in-plane deformation of monosubstituted benzene rings. The peaks at 755 and 696 cm^{-1} were due to the out-of-plane deformation vibrations of styrene. The presence of these characteristic peaks in the FTIR spectra of different PSt-based microspheres were due to the benzene ring, methyl, and methylene groups. These results were consistent with previous studies [35,38].

When copolymers were added to the emulsion polymerization, microspheres containing different polymers such as polymethyl methacrylate (PMMA), polybutyl acrylate (PBA), and polyacrylic acid (PAA), were obtained. This caused differences in FTIR spectra between synthesized microspheres of copolymers and those of pure PSt microspheres. P(St-AA), P(St-MMA-AA), and P(St-BA-AA) microspheres showed a characteristic peak at 1703 cm^{-1}, corresponding to the stretching vibrations of C=O. This indicated that hydrophilic carboxyl groups were introduced into microspheres due to copolymerization of AA with St. Moreover, the characteristic peak of P(St-AA) microspheres at 1703 cm^{-1} was most obvious among the above three copolymers, due to the absence of MMA and BA [16]. The introduction of carboxyl groups made microspheres more hydrophilic, and the hydrogen bonds of carboxyl groups would enhance the linkage of microspheres and contribute to the formation of coatings with a structural color. For the four microspheres obtained by copolymerization with MMA and BA, a peak at 1729 cm^{-1} was ascribed to the stretching vibrations of C=O in esters. The spectra of P(St-MMA-AA) and P(St-MMA) microspheres showed additional characteristic peaks at 1196 and 1114 cm^{-1}, respectively.

These two peaks were the result of symmetric stretching vibrations of C–O–C in MMA, which indicated successful copolymerization between MMA and St. A peak at 1156 cm^{-1} in the case of P(St-BA-AA) and P(St-BA) increased in intensity due to the introduction of C–O–C, which demonstrated the successful copolymerization of BA with St.

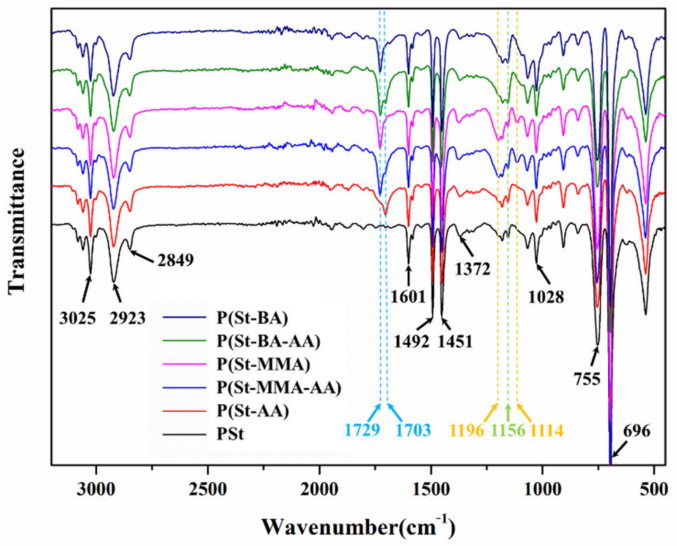


Figure 3. FTIR spectra of PSt-based microspheres.

3.1.3. TEM Analysis of Microspheres of Different PSt Copolymers

TEM images of six PSt-based colloidal microspheres are shown in Figure 4. The particle sizes of all microspheres synthesized by an emulsion polymerization method in this paper were significantly different. However, diameters of PSt and P(St-BA) microspheres (Figure 4a,f) were almost identical. Measurements of 100 microspheres in different TEM images for each of the copolymers showed that the particle sizes of these two microspheres were about 227 nm. However, these two kinds of microspheres had obviously different structures. PSt microspheres (Figure 4a) showed uniform morphology, while P(St-BA) microspheres (Figure 4f) showed core–shell morphology [26,39]. It was speculated that the core of P(St-BA) was a PSt hard microsphere, with a soft PBA shell of about 50 nm thickness wrapped around it. The addition of MMA, BA, and AA as comonomers also resulted in their microspheres having core–shell morphologies, but with differences in particle sizes. In terms of morphology, the surfaces of three types of colloidal microspheres, P(St-AA), P(St-MMA-AA), and P(St-BA-AA) (Figure 4b,c,e), with AA as comonomer, were not smooth in the TEM images, especially for P(St-AA) microspheres. It could be inferred that this phenomenon was mainly dependent on the properties of PAA on the surface layer of microspheres. The polymerization of acrylic acid (possessing a –COOH group) on the surface of the PSt core to form macromolecular chains produced a PAA layer that was rubbery. When microspheres with this core–shell morphology were dispersed in the emulsion, the shell of the microsphere swelled. During sample preparation for TEM, the diluted emulsion containing microspheres was dripped onto copper mesh, followed by drying of the emulsion by light irradiation. The microspheres continuously lost water, due to which the swollen part coalesced and developed into a rough and laminated surface.

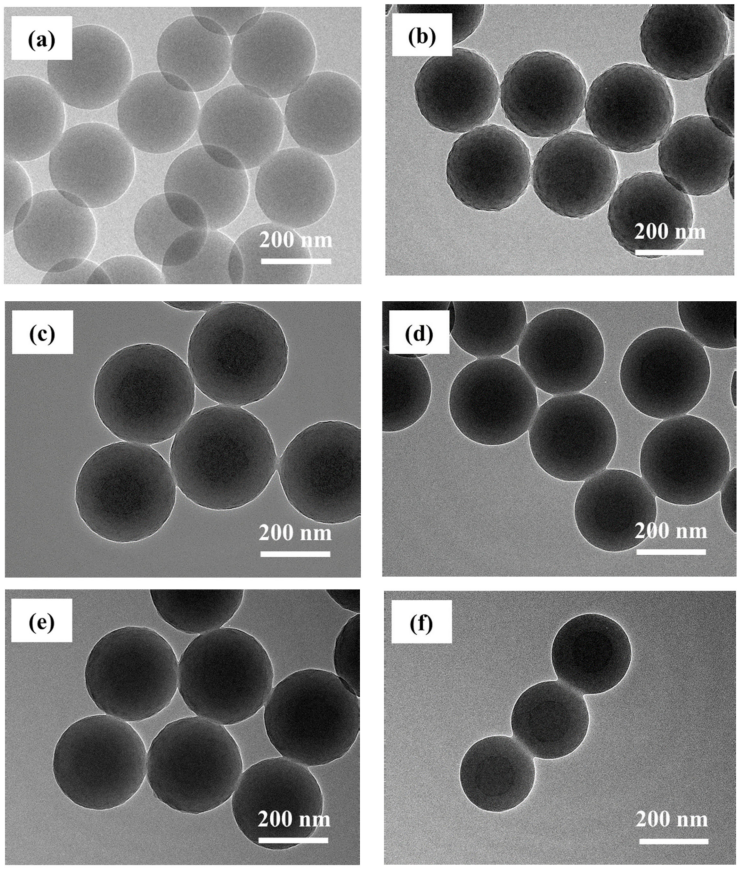


Figure 4. TEM images of PSt-based microspheres; (**a**) PSt, (**b**) P(St-AA), (**c**) P(St-MMA-AA), (**d**) P(St-MMA), (**e**) P(St-BA-AA), and (**f**) P(St-BA).

3.2. Effect of Copolymer Composition on Properties of Coatings on a Wood Surface

3.2.1. SEM of Coatings on a Wood Surface

Figure 5 shows top view morphologies of the coatings formed from colloidal microspheres of PSt and PSt-based copolymers on a wood surface at 50 °C. It can be seen that irrespective of the type of copolymer, the particle sizes of microspheres in each coating were different, that is, the monodispersity was poor. However, among all the SEM images, P(St-AA) microspheres showed good monodispersity. The average particle size of 100 microspheres was found to be about 238 nm. The microstructure of the coating formed on the wood surface appeared to be well ordered, and colloidal microspheres were closely arranged into a neat hexagonal structure, representing the (111) crystal surfaces of a face center cubic (fcc) structure [14,16,17]. Since P(St-AA) microspheres had a flexible shell structure comprising PAA, microspheres squeezed each other and the soft shell underwent deformation during the self-assembly process. The spheres changed from a spherical to an approximately hexagonal shape, resulting in a more compact arrangement of the photonic crystal structure.

Coatings made from P(St-MMA) and P(St-BA-AA) colloidal microspheres also displayed a locally ordered structure (Figure 5d,e). Microspheres were mainly arranged in the form of dense hexagonal arrangements, but some positions were defective, which could have been caused for two reasons. On one hand, there were some microspheres whose particle sizes were obviously smaller than the average. These microspheres participated in self-assembly but could not form a highly well-ordered photonic crystal structure. On the other hand, in the self-assembly process of thermally assisted gravity deposition, under the action of heat, microspheres firstly aggregated on the emulsion surface into pieces of a densely arranged hexagonal crystal structure. Then, with the evaporation of dispersant, the small pieces of crystals were gradually gathered. Due to interspatial hindrances,

a defect-free long-range ordered photonic crystal structure could not be accurately formed, resulting in cracks and dislocation [40,41].

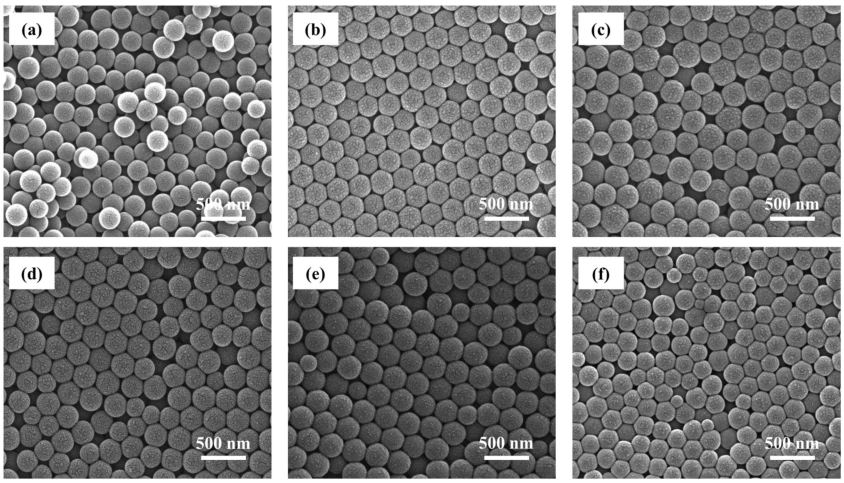


Figure 5. Top view of the morphologies and structures of coatings formed by self-assembly of PSt-based microspheres on a wood surface at 50 °C; (**a**) PSt, (**b**) P(St-AA), (**c**) P(St-MMA-AA), (**d**) P(St-MMA), (**e**) P(St-BA-AA), and (**f**) P(St-BA).

However, the surface microstructure of coatings from PSt, P(St-MMA-AA), and P(St-BA) microspheres were less ordered and their surface structures were not dense (Figure 5a,c,f). More isolated microspheres appeared on the surface coating made from PSt microspheres (Figure 5a). Meanwhile, aggregated microspheres were not well ordered and resulted in an amorphous nature of the photonic crystal. SEM images also showed that the surface of pure PSt colloidal microspheres was smoother than those of the colloidal microspheres of copolymers, but extrusion deformation between aggregated microspheres was still present. It was evident from this study that the monodispersities of P(St-MMA-AA) and P(St-BA) colloidal microspheres (Figure 5c,f) were poor and there are many microspheres whose diameters were smaller than the average diameters. This reduced the area of the ordered arrangement of coatings for these two kinds of microspheres, wherein the microspheres became more irregular during the extrusion process. These factors weakened the band gap of photonic crystals.

It is worth noting that wood is formed by kinds of cells which make wood different from other homogeneous substrate materials such as glass, silicon, and metal. This results in micron-scale roughness of the wood surface. The roughness of the substrate is significant for the self-assembly of photonic crystals, and the roughness of the heterogeneous material wood is crucial due to the high surface complexity (anatomy, chemistry). In this study, the wood of aspen (Populus tremuloides) is light, soft, and straight grained. It has good dimensional stability and it turns, sands, and holds glue and paint well. It has relatively low strength, however, and is moderately low in shock resistance. The wood substrate surface was polished with 320-mesh sandpaper due to the obvious revolution marks, burrs, and roughness on the wood surface after being sawn, which will affect the formation of photonic crystals on the wood surface. Sanding will significantly improve the surface roughness of wood. The surface of sanded wood blocks was smooth and clean, and the parallel linear textures and fine xylem ray can be clearly observed on the wood surface.

The species of wood, coniferous or broad-leaved wood, macroscopic and microscopic anatomical features of wood, the type of wood cell, quarter-sawed lumber or plain-sawed lumber, and chemical properties of wood will affect the formation of photonic crystals. The future research direction of our research group is to construct photonic crystals with high performance on wood surfaces with micron-level roughness. Some of the factors mentioned above have been studied, and the results will be analyzed and discussed in other papers.

3.2.2. Reflectance Spectroscopy of Coatings on a Wood Surface

In this study, optical properties of coatings on the wood surface were characterized by UV–Vis reflectance spectroscopy. The effect of temperature on the optical property during thermally assisted gravity deposition was compared. In Figure 6, reflectance spectra of coatings formed by the self-assembly of PSt-based colloidal microspheres on a wood surface at 40, 50, 60, and 70 °C are shown. Microsphere size directly affects the three-dimensional structure of photonic crystals, consisting of microspheres and air cavities. This then influences the band gap characteristics, which is in accordance with Bragg's diffraction equation [24,33,36]. As shown in Figure 6a,f, particle sizes of PSt and P(St-BA) colloidal microspheres, synthesized in this study, were about 210–230 nm. Moreover, the peak of photonic crystal formed by self-assembly of these two kinds of microspheres at 40 °C appeared at about 490 nm. However, the relationship between reflectance peak and the temperature of the self-assembly process of these two different microspheres was not the same. The positions of the reflectance peak of coatings formed by PSt microspheres increased with self-assembly temperature and were red shifted. However, when the temperature of self-assembly increased, the positions of the visible light reflectance peaks of the coatings of P(St-BA) microspheres were constant. This phenomenon may be related to the soft properties of PBA.

Particle sizes of P(St-AA) and P(St-MMA) colloidal microspheres (Figure 5b,d) were similar, about 235–255 nm. For photonic crystal coatings of P(St-AA) microspheres, when the self-assembly temperatures were 40, 50, and 60 °C, peaks of visible light reflection appeared at 593 nm. However, as the temperature was continuously raised to 70 °C, the reflectance peak of the coating was blue shifted to about 578 nm. For all the above four coatings, at a self-assembly temperature of 50 °C, their peak positions were the same and the relative peak height of the reflectivity curve was the maximum. Hence, at this temperature, the photonic crystal structures formed by these four types of colloidal microspheres by thermally assisted gravity deposition showed the strongest response to the corresponding wavelength and the structures of these coatings were more ordered.

In contrast to the above phenomenon, the relative peak heights of the reflectivity curve for P(St-MMA-AA) and P(St-BA-AA) coatings were the maximum, when self-assembled at 40 °C, as shown in Figure 6c,e. Additionally, these two microspheres also had similar particle sizes of about 260–265 nm. For P(St-MMA-AA) coatings, the position of the reflectance peak showed a red shift from 593 to 610 nm with an increase in self-assembly temperature. However, for P(St-BA-AA) coatings, when the self-assembly temperature was 40 °C, the reflectance peak was 613 nm. With an increase in self-assembly temperature, the reflectance peaks of coatings were blue shifted. For coatings formed at 50, 60, and 70 °C, the reflectance peaks appeared at 589 nm.

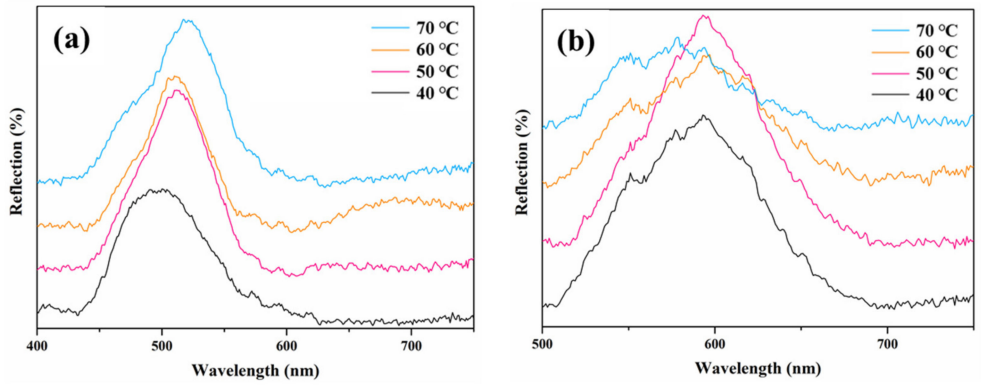


Figure 6. *Cont.*

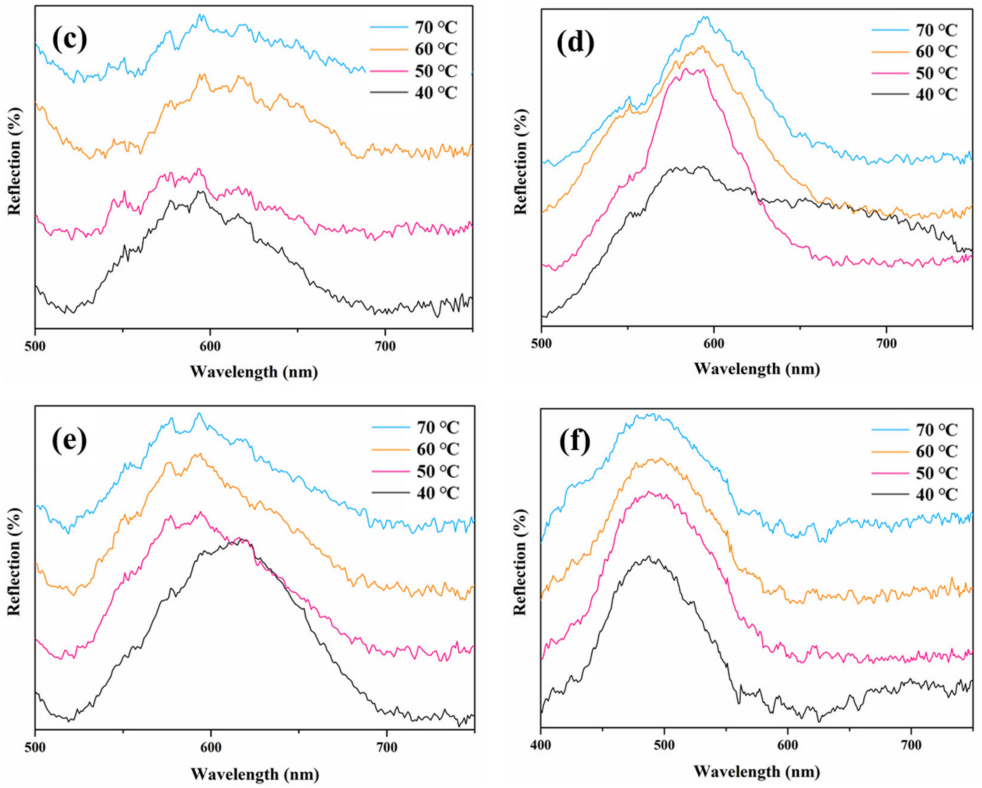


Figure 6. Reflectance spectra of coatings formed by self-assembly of PSt-based colloidal microspheres on a wood surface at 40, 50, 60, and 70 °C; (**a**) PSt, (**b**) P(St-AA), (**c**) P(St-MMA-AA), (**d**) P(St-MMA), (**e**) P(St-BA-AA), and (**f**) P(St-BA).

3.2.3. Structural Colors of Coatings on a Wood Surface

Figure 7 shows the structural colors of coatings formed by PSt-based colloidal microspheres on a wood surface, under white light irradiation. The images of structural colors of coatings were consistent with the results of spectral analysis of visible light reflectance in Section 3.2.2. The color of coatings formed by PSt and P(St-BA) colloidal microspheres was green, which corresponded to the reflectance peak at 490 nm. When the temperatures of self-assembly were 40, 50, and 60 °C, the coatings formed by PSt microspheres could not cover the area of emulsion drop evenly and completely, and the structural color was shown as bright green. Colloidal microspheres gathered during self-assembly, and due to the coffee ring effect, the microspheres first aggregated close to edge of the coated region. This study found that when the coating area was fixed, irrespective of whether the amount of emulsion or solid content in the emulsion was adjusted, the coatings could not completely cover the fixed area. However, this phenomenon did not occur when the self-assembly temperature was raised to 70 °C. Coatings constructed at this temperature could almost cover the entire area of the emulsion drop, and the changes in structural color of the coating were also consistent with the red shift of the reflection peak with temperature. When the self-assembly temperature was raised from 40 to 70 °C, the structural colors of the coatings gradually changed from green to yellowish green. This may be related to the number of layers of long-range ordered photonic crystals in coatings.

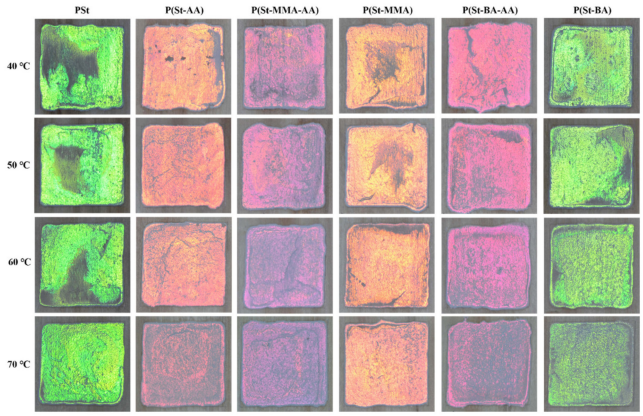


Figure 7. Images of as-prepared coatings of PSt-based colloidal microspheres on a wood surface, under white light illumination.

Although coatings formed from P(St-BA) microspheres could also not cover the entire coating area, it was not as obvious as for PSt coatings. The structural colors of coatings did not change significantly with an increase in self-assembly temperature. For these two kinds of microspheres, when the self-assembly temperature was 50 °C, the coatings showed the strongest light reflection. The picture displayed higher brightness, which implied that the coatings formed at this temperature had a more well-ordered photonic crystal structure. When P(St-BA) coatings were developed at 60 and 70 °C, the color saturation of the coatings was very low, and the peak height of relative reflectivity in the reflectance spectrum was less. This phenomenon may be caused by thermal softening of PBA or an increase in the disordered structure.

When self-assembly temperatures were 40, 50, and 60 °C, the structural colors of P(St-AA) coatings were orange. According to SEM analysis, colloidal microspheres had good monodispersity and a well-ordered structure, and hence the color saturation was high. When the self-assembly temperature was 70 °C, the color of coating became very dim, which could be due to rapid evaporation of the emulsion dispersant and disordered accumulation of colloidal microspheres on the wood surface, prior to orderly arrangement. The structural color of P(St-MMA) coatings was orange–yellow and the thickness of coatings formed at 40 and 50 °C was uneven. With an increase in self-assembly temperature, the color of P(St-MMA) coatings gradually changed to orange, which was consistent with the red shift in the reflectance spectrum. P(St-MMA-AA) and P(St-BA-AA) coatings showed a pink structural color. However, P(St-BA-AA) microspheres had better monodispersity, and the arrangement of microspheres was more orderly in the coatings formed, and so color saturation was higher. The most brilliant color of these two coatings was obtained when the self-assembly temperature was 40 °C, which was consistent with the results of reflectance spectroscopy. The red or blue shift of reflectance peaks with temperature could be the result of effective changes in the crystal structure of coatings with an increase in temperature during the self-assembly process.

4. Conclusions

In conclusion, six kinds of PSt-based colloidal microspheres were synthesized by emulsion polymerization by using different comonomers. These coatings were self-assembled by the thermally assisted gravity deposition method on a wood surface. Among them, pure PSt colloidal microspheres were homogeneous, and the surface showed the presence of oxygen due to APS and SDBS. The other colloidal microspheres of copolymers had core–shell morphologies. The peak intensity of O element in XPS spectra was relatively improved due to the addition of AA, MMA, and BA. FTIR results showed that copolymeric microspheres contained an abundant number of C=O groups. Not all kinds of colloidal microspheres had monodispersity, and hence the microstructures of coatings formed by the self-assembly of microspheres on the wood surface were not orderly over a long range, but

could still produce bright structural colors. There was a correlation between the position of the reflectance peak and the particle size of coatings. With an increase in particle size, the wavelength of the reflectance peak was red shifted. The formulations and reaction conditions used for emulsion polymerization in this paper will be further optimized in future research work.

Author Contributions: Conceptualization, Y.L.; methodology, Y.L. and J.H.; data curation, Y.L.; writing—original draft preparation, Y.L.; writing—review and editing, Y.L.; visualization, J.H. All authors have read and agreed to the published version of the manuscript.

Funding: This work was supported by the Youth Program of the Science and Technology Innovation Fund of Nanjing Forestry University (Grant No. CX2019016) and the Scientific Research Foundation of Nanjing Forestry University (Grant No. GXL 2018022).

Data Availability Statement: The raw and processed data required to reproduce these findings cannot be shared at this time as the data also forms part of an ongoing study.

Acknowledgments: The authors are grateful for financial support from the Youth Program of the Science and Technology Innovation Fund of Nanjing Forestry University (Grant No. CX2019016) and the Scientific Research Foundation of Nanjing Forestry University (Grant No. GXL 2018022).

Conflicts of Interest: The authors declare no conflict of interest.

References

1. Xiong, X.; Ma, Q.; Yuan, Y.; Wu, Z.; Zhang, M. Current situation and key manufacturing considerations of green furniture in China: A review. *J. Clean Prod.* **2020**, *267*, 121957. [CrossRef]
2. Yang, L.; Liu, H. Effect of a combination of moderate-temperature heat treatment and subsequent wax impregnation on wood hygroscopicity, dimensional stability, and mechanical properties. *Forests* **2020**, *11*, 920. [CrossRef]
3. Bekhta, P.; Niemz, P. Effect of high temperature on the change in color, dimensional stability and mechanical properties of spruce wood. *Holzforschung* **2003**, *57*, 539–546. [CrossRef]
4. Hansmann, C.; Deka, M.; Wimmer, R.; Gindl, W. Artificial weathering of wood surfaces modified by melamine formaldehyde resins. *Eur. J. Wood Wood Prod.* **2006**, *64*, 198–203. [CrossRef]
5. Liu, Y.; Shao, L.; Gao, J.; Guo, H.; Chen, Y.; Chen, Q.; Via, B.K. Surface photo-discoloration and degradation of dyed wood veneer exposed to different wavelengths of artificial light. *Appl. Surf. Sci.* **2015**, *331*, 353–361. [CrossRef]
6. Robinson, S.C.; Hinsch, E.; Weber, G.; Leipus, K.; Cerney, D. Wood colorization through pressure treating: The potential of extracted colorants from spalting fungi as a replacement for woodworkers' aniline dyes. *Materials* **2014**, *7*, 5427–5437. [CrossRef] [PubMed]
7. Gutierrez, S.M.V.; Robinson, S.C. Microscopic analysis of pigments extracted from spalting fungi. *J. Fungi* **2017**, *3*, 15. [CrossRef] [PubMed]
8. Hinsch, E.M.; Robinson, S.C. Comparing colorfastness to light of wood-staining fungal pigments and commercial dyes: An alternative light test method for color fastness. *Coatings* **2018**, *8*, 189. [CrossRef]
9. Huang, X.; Kocaefe, D.; Kocaefe, Y.; Boluk, Y.; Pichette, A. A spectrocolorimetric and chemical study on color modification of heat-treated wood during artificial weathering. *Appl. Surf. Sci.* **2012**, *258*, 5360–5369. [CrossRef]
10. Wang, X.; Tang, R.; Zhang, Y.; Yu, Z.; Qi, C. Preparation of a novel chitosan-based biopolymer dye and application in wood dyeing. *Polymers* **2016**, *8*, 338. [CrossRef]
11. Zi, J.; Yu, X.; Li, Y.; Hu, X.; Xu, C.; Wang, X.; Liu, X.; Fu, R. Coloration strategies in peacock feathers. *Proc. Natl. Acad. Sci. USA* **2003**, *100*, 12576–12578. [CrossRef] [PubMed]
12. Kolle, M.; Lethbridge, A.; Kreysing, M.; Baumberg, J.J.; Aizenberg, J.; Vukusic, P. Bio-inspired band-gap tunable elastic optical multilayer fibers. *Adv. Mater.* **2013**, *25*, 2239–2245. [CrossRef]
13. Parker, A.R. Colour in Burgess Shale animals and the effect of light on evolution in the Cambrian. *Proc. R. Soc. B Biol. Sci.* **1998**, *265*, 967–972. [CrossRef]
14. Pusey, P.N.; Van Megen, W.; Bartlett, P.; Ackerson, B.J.; Rarity, J.G.; Underwood, S.M. Structure of crystals of hard colloidal spheres. *Phys. Rev. Lett.* **1989**, *63*, 2753–2756. [CrossRef] [PubMed]
15. Saranathan, V.; Osuji, C.; Mochrie, S.; Noh, H.; Narayanan, S. Crystals in butterfly wing scales. *Proc. Natl. Acad. Sci. USA* **2010**, *107*, 11676–11681. [CrossRef] [PubMed]
16. Wang, J.; Wen, Y.; Ge, H.; Sun, Z.; Zheng, Y.; Song, Y.; Jiang, L. Simple fabrication of full color colloidal crystal films with tough mechanical strength. *Macromol. Chem. Phys.* **2006**, *207*, 596–604. [CrossRef]
17. Aguirre, C.I.; Reguera, E.; Stein, A. Colloidal photonic crystal pigments with low angle dependence. *ACS Appl. Mater. Inter.* **2010**, *2*, 3257–3262. [CrossRef]
18. Vigneron, J.P.; Simonis, P. Natural photonic crystals. *Physica B* **2012**, *407*, 4032–4036. [CrossRef]

19. Chen, J.; Xie, J.; Wu, Z.; Elbashiry, E.M.A.; Lu, Y. Review of beetle forewing structures and their biomimetic applications in China: (I) On the structural colors and the vertical and horizontal cross-sectional structures. *Mat. Sci. Eng. C Mater.* **2015**, *55*, 605–619. [CrossRef]
20. Wong, S.; Kitaev, V.; Ozin, G.A. Colloidal crystal films: Advances in universality and perfection. *J. Am. Chem. Soc.* **2003**, *125*, 15589–15598. [CrossRef]
21. Cheng, B.; Ni, P.; Jin, C.; Li, Z.; Zhang, D.; Dong, P.; Guo, X. More direct evidence of the fcc arrangement for artificial opal. *Opt. Commun.* **1999**, *170*, 41–46. [CrossRef]
22. Stöber, W.; Fink, A.; Bohn, E. Controlled growth of monodisperse silica spheres in the micron size range. *J. Colloid. Interf. Sci.* **1968**, *26*, 62–69. [CrossRef]
23. Lei, X.; Yu, B.; Cong, H.; Tian, C.; Wang, Y.; Wang, Q.; Liu, C. Synthesis of monodisperse silica microspheres by a modified Stöber method. *Integr. Ferroelectr.* **2014**, *154*, 142–146. [CrossRef]
24. You, B.; Wen, N.; Shi, L.; Wu, L.; Zi, J. Facile fabrication of a three-dimensional colloidal crystal film with large-area and robust mechanical properties. *J. Mater. Chem.* **2009**, *19*, 3594–3597. [CrossRef]
25. Zhang, S.; Chen, J.; Taha, M. Synthesis of monodisperse styrene/methyl methacrylate/acrylic acid latex using surfactant-free emulsion copolymerization in air. *J. Appl. Polym. Sci.* **2009**, *114*, 1598–1605. [CrossRef]
26. Shen, Z.; Yang, Y.; Lu, F.; Bao, B.; You, B. Self-assembly of binary particles and application as structural colors. *Polym. Chem.* **2012**, *3*, 2495–2501. [CrossRef]
27. Liu, G.; Zhou, L.; Zhang, G.; Li, Y.; Chai, L.; Fan, Q.; Shao, J. Fabrication of patterned photonic crystals with brilliant structural colors on fabric substrates using ink-jet printing technology. *Mater. Design* **2017**, *114*, 10–17. [CrossRef]
28. Xu, L.; Li, H.; Jiang, X.; Wang, J.; Li, L.; Song, Y.; Jiang, L. Synthesis of amphiphilic mushroom cap-shaped colloidal particles towards fabrication of anisotropic colloidal crystals. *Macromol. Rapid Comm.* **2010**, *31*, 1422–1426. [CrossRef]
29. Kang, K.; Kan, C.; Du, Y.; Liu, D. Synthesis and properties of soap-free poly(methyl methacrylate-ethyl acrylate-methacrylic acid) latex particles prepared by seeded emulsion polymerization. *Eur. Polym. J.* **2005**, *41*, 439–445. [CrossRef]
30. Kim, S.H.; Son, W.K.; Kim, Y.J.; Kang, E.G.; Kim, D.W.; Park, C.W.; Kim, W.G.; Kim, H.J. Synthesis of polystyrene/poly(butylacrylate) core–shell latex and its surface morphology. *J. Appl. Polym. Sci.* **2003**, *88*, 595–601. [CrossRef]
31. Hoshino, F.; Kawaguchi, H.; Ohtsuka, Y. N-substituted acrylamide-styrene copolymer lattices III. Morphology of latex particles. *Polym. J.* **1987**, *19*, 1157–1164. [CrossRef]
32. Kim, S.; Seo, Y.G.; Cho, Y.; Shin, J.; Gil, S.C.; Lee, W.M. Optimization of emulsion polymerization for submicron-sized polymer colloids towards tunable synthetic opals. *Bull. Korean. Chem. Soc.* **2010**, *31*, 1891–1896. [CrossRef]
33. Zhao, T.; Zhang, Y.; Wang, J.; Song, Y.; Jiang, L. Fabrication of phase-change polymer colloidal photonic crystals. *J. Nanomater.* **2014**, *4*, 702089. [CrossRef]
34. Sun, C.; Yao, Y.; Gu, Z. Fabrication of elastic colloidal crystal films from pure soft spheres. *Colloid. Surface. A* **2012**, *402*, 102–107. [CrossRef]
35. Wang, J.; Wen, Y.; Feng, X.; Song, Y.; Jiang, L. Control over the wettability of colloidal crystal films by assembly temperature. *Macromol. Rapid. Comm.* **2006**, *27*, 188–192. [CrossRef]
36. Liu, G.; Shao, J.; Zhang, Y.; Wu, Y.; Wang, C.; Fan, Q.; Zhou, L. Self-assembly behavior of polystyrene/methacrylic acid (P(St-MAA)) colloidal microspheres on polyester fabrics by gravitational sedimentation. *J. Text. Inst.* **2015**, *106*, 1293–1305. [CrossRef]
37. Wang, P.H.; Pan, C.Y. Emulsion copolymerization of styrene with acrylic or methacrylic acids-distribution of the carboxylic group. *Colloid Polym. Sci.* **2001**, *279*, 98–103. [CrossRef]
38. Zhang, Y.; Hao, X.; Zhou, J.; Zhang, Y.; Wang, J.; Song, Y.; Jiang, L. Tough and hydrophilic photonic crystals obtained from direct UV irradiation. *Macromol. Rapid Comm.* **2010**, *31*, 2115–2120. [CrossRef]
39. Wang, J.; Wen, Y.; Hu, J.; Song, Y.; Jiang, L. Fine control of the wettability transition temperature of colloidal-crystal films: From superhydrophilic to superhydrophobic. *Adv. Funct. Mater.* **2007**, *17*, 219–225. [CrossRef]
40. Huang, Y.; Zhou, J.; Su, B.; Shi, L.; Wang, J.; Chen, S.; Wang, L.; Zi, J.; Song, Y.; Jiang, L. Colloidal photonic crystals with narrow stopbands assembled from low-adhesive superhydrophobic substrates. *J. Am. Chem. Soc.* **2012**, *134*, 17053–17058. [CrossRef]
41. Zhou, J.; Wang, J.; Huang, Y.; Liu, G.; Wang, L.; Chen, S.; Li, X.; Wang, D.; Song, Y.; Jiang, L. Large-area crack-free single-crystal photonic crystals via combined effects of polymerization-assisted assembly and flexible substrate. *NPG Asia Mater.* **2012**, *4*, e21. [CrossRef]